




REVIEW ARTICLE

<https://doi.org/10.1038/s41467-019-11450-z>

OPEN

Subseafloor life and its biogeochemical impacts

Steven D'Hondt ¹, Robert Pockalny ¹, Victoria M. Fulfer ¹ & Arthur J. Spivack¹

Subseafloor microbial activities are central to Earth's biogeochemical cycles. They control Earth's surface oxidation and major aspects of ocean chemistry. They affect climate on long timescales and play major roles in forming and destroying economic resources. In this review, we evaluate present understanding of subseafloor microbes and their activities, identify research gaps, and recommend approaches to filling those gaps. Our synthesis suggests that chemical diffusion rates and reaction affinities play a primary role in controlling rates of subseafloor activities. Fundamental aspects of subseafloor communities, including features that enable their persistence at low catabolic rates for millions of years, remain unknown.

Subseafloor ecosystems constitute a significant portion of Earth's biosphere. The estimated total number of cells in marine sediment ($\sim 10^{29}$)¹ rivals estimated totals in the ocean and in soil². Although total cell abundance is unknown for the igneous aquifer that underlies marine sediment, microbes are routinely recovered from this aquifer³, chemical traces of their activity are pervasive in its altered rock^{4,5} and formation fluid⁶, and physical textures suggestive of microbial alteration are common⁷. The total volume of subseafloor habitats is immense; the volumes of marine sediment and igneous basement cooler than 122 °C [the currently accepted high-temperature limit to life⁸] are respectively $2.6 \times 10^8 \text{ km}^3$ ⁹ and $1.0 \times 10^9 \text{ km}^3$ (Methods). The volumes of potentially habitable void space within the sediment⁹ and basement, respectively, are about $8.5 \times 10^7 \text{ km}^3$ and $8.0 \times 10^7 \text{ km}^3$ (each equal to about 6% of ocean volume [$1.3 \times 10^9 \text{ km}^3$]¹⁰).

Mean respiration per cell is very low in subseafloor sediment^{11,12}. Although their total abundance is high, microbial cells in marine sediment are generally much smaller than microbial cells in the surface world. Consequently, the total biomass of marine sedimentary life is <1% of Earth's total biomass¹. Per-cell catabolic rates and total biomass are presently unknown for microbial communities in the igneous aquifer beneath the sediment.

Because subseafloor communities reside at the interface between the biologically active surface world and the large geological reservoirs of biologically important chemicals, subseafloor microbial activities play a fundamental role in Earth's biogeochemical cycles. This role is particularly visible in the organic-fueled activity of marine sedimentary life. Burial of reducing power (electron donors) in the form of organic matter and pyrite (FeS_2) is the principal driver of Earth's surface oxidation over geologic time¹³. Subseafloor life is the last biological filter through which organic matter passes on its way to burial and subduction. Among Earth's surface and near-surface environments, marine sediment is the largest reservoir of carbon (including both the reduced carbon in organic matter and the oxidized carbon in sedimentary carbonates)¹⁴ and the third largest reservoir of nitrogen (after the atmosphere and continental crust)¹⁵.

The general geography of subseafloor catabolic activity is well constrained. Anaerobic activity dominates in the fast-accumulating sediment of continental margins and oceanic upwelling

¹ Graduate School of Oceanography, University of Rhode Island Narragansett Bay Campus, 215 South Ferry Road, Rhode Island 02882, USA. Correspondence and requests for materials should be addressed to S.D. (email: dhondt@uri.edu)

regions, where seafloor respiration greatly outpaces the flux of dissolved oxygen (O_2) into the sediment from the ocean. Aerobic activity dominates in the very slowly accumulating sediment of the deep open ocean, where seafloor respiration rates are very low and the O_2 flux keeps pace with respiration throughout the sediment column¹⁶ (Fig. 1). Rates of organic activity are highest in young, near-seafloor sediment and decline rapidly with increasing depth below seafloor¹⁷ (Fig. 2). Similarly, oxidation of igneous ocean crust is fastest for young crust (less than circa 10 Ma) and relatively slow thereafter¹⁸. Crustal oxidation is generally greatest where permeability is highest and seawater flow through the igneous aquifer is consequently fastest¹⁹. This is typically in discrete zones within the upper 200–500 m of the igneous sequence²⁰ (Fig. 3).

Given the ubiquity of seafloor life and its central role in chemical exchange between the surface and subsurface worlds, this review has three major objectives. The first objective is to synthesize present understanding of seafloor microbes, their catabolic activities, and their global consequences. The second objective is to advance understanding of the factor(s) that ultimately limit rates of seafloor activities. The third objective is to identify major gaps in scientific understanding of seafloor communities and activities, and recommend approaches to filling those gaps.

Diversities of seafloor organisms and activities. Seafloor sediment and the underlying basaltic aquifer are inhabited by many lineages of Bacteria^{21–23}, Archaea^{22,23}, and a subset of the Eukarya (fungi)^{24,25}. Transcriptional data indicate that members of all three domains are active in seafloor sediment²⁵. Viruses

are also abundant in both the sediment²⁶ and the basaltic aquifer²⁷.

Due to low per-cell energy fluxes²⁸, selection is fierce in seafloor sediment, leading both microbial diversity²⁹ and cell concentration¹ to decline exponentially with sediment depth and age. Broadly defined taxonomic groups (*Chloroflexi*, *Deltaproteobacteria*, *Firmicutes*) are present in relatively cool seafloor sediment throughout much of the ocean^{22,23,29–34}, suggesting that the consequences of this selection are relatively consistent at coarse taxonomic levels.

Geographic distributions of taxonomic richness and microbial abundance are largely unknown for the seafloor igneous aquifer. However, different habitats within this environment are known to harbor distinctly different communities. For example, hot (65 °C) anoxic fluid in 3.5-Ma basalt of the Juan de Fuca Ridge (northeastern Pacific) contains abundant thermophilic anaerobes^{3,35}, while relatively cold (3–4 °C) oxic fluid of the North Pond aquifer (central North Atlantic) is dominated by diverse *Proteobacteria*^{36,37}. Communities from both aquifers are dominated by bacteria, with only trace concentrations of archaea^{35,37}.

Seafloor organisms glean energy from a broad range of redox reactions (e.g., disproportionation reactions, such as fermentation, and respiration reactions). In both the sediment and the igneous basement, electron acceptors (oxidants) for respiration include dissolved chemicals (O_2 , nitrate [NO_3^-], sulfate [SO_4^{2-}]) carried by diffusion or flow into the seafloor, oxidized elements in minerals, and hydrogen peroxide (H_2O_2) from water radiolysis. In sediment, electron donors (reductants) include organic matter and reduced minerals deposited from the

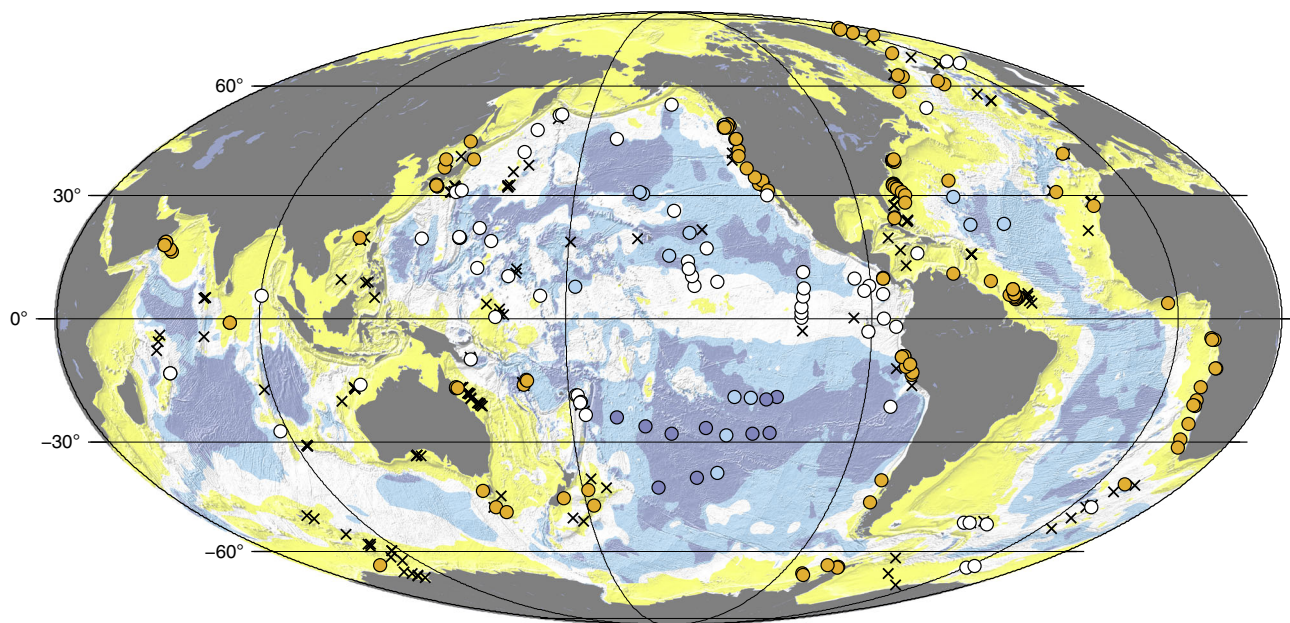


Fig. 1 Global distributions of dissolved O_2 and SO_4^{2-} in seafloor sediment. In yellow regions, dissolved SO_4^{2-} is expected to disappear within the sediment and HCO_3^- is expected to be the predominant net electron acceptor at greater depths. In white regions, dissolved SO_4^{2-} is expected to penetrate throughout the sediment, from seafloor to igneous basement. Dark blue and light blue regions respectively represent the minimum and maximum areas over which dissolved O_2 is expected to penetrate throughout the sediment from seafloor to basement¹⁶. SO_4^{2-} reduction is expected to dominate net seafloor organic oxidation in the yellow and white regions. O_2 reduction is expected to dominate net seafloor organic oxidation in the blue regions. Orange dots mark drill sites where SO_4^{2-} disappears within the first 500 meters of sediment. White dots mark drill sites where SO_4^{2-} penetrates the entire sediment sequence. Dark blue dots mark drill sites where dissolved O_2 and dissolved SO_4^{2-} penetrate the entire sediment sequence. Medium blue dots mark coring sites where O_2 and SO_4^{2-} penetrate to the bottom of the cores (meters to tens of meters) and may penetrate to basement. X symbols mark sites where the full extent of SO_4^{2-} penetration is unknown, because SO_4^{2-} is present in all measured samples, but the sedimentary sequence continues far below the last measurement. More information regarding the generation of this map is available in the Methods section

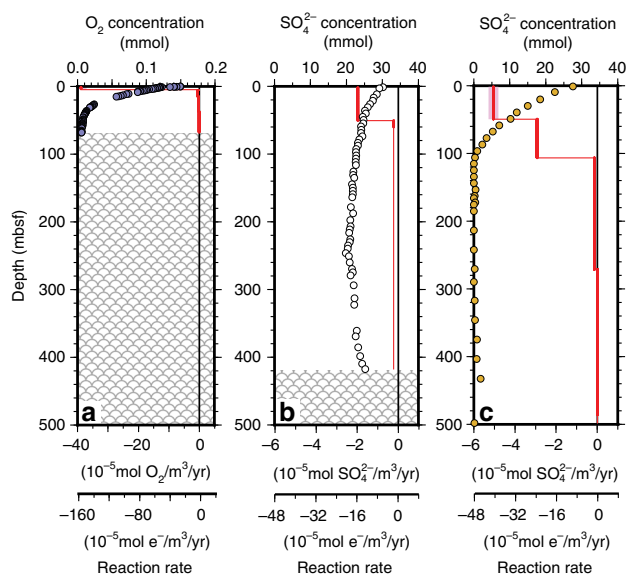


Fig. 2 Profiles of net respiration rates at representative sites. **a** Profile of net respiration rate (O_2 reduction rate) as a function of sediment depth at oxic IODP Site U1370 (dark blue zone in Fig. 1). **b** Profile of net respiration rate (SO_4^{2-} reduction rate) as a function of sediment depth at anoxic ODP Site 1226, where dissolved SO_4^{2-} is present throughout the sediment column (white zone in Fig. 1). **c** Profile of net respiration rate (SO_4^{2-} reduction rate) as a function of sediment depth at anoxic ODP Site 984, where dissolved SO_4^{2-} is depleted at a relatively shallow sediment depth (yellow zone in Fig. 1). Circles mark chemical concentration data color-coded to the Fig. 1 geographic zones in which the sites occur (dark blue, white and yellow, respectively). Red lines mark net respiration rates and pink bars mark uncertainty (first standard deviation). Crosshatched zones in A and B mark igneous basement

overlying world²⁸, and hydrogen (H_2) from in situ radiolysis of water³⁸. In the igneous crust, electron donors include reduced elements in the rock (which originated in the underlying mantle)¹⁸, dissolved organic matter that enters with water from the overlying ocean⁶, and H_2 from in situ water radiolysis³⁹. Although in situ radiolysis may support subsurface respiration in both the sediment and the underlying igneous aquifer, it may not have a net effect on subsurface chemistry or global biogeochemical cycles, because it simultaneously creates reductant (H_2) and oxidant (H_2O_2 and oxidized mineral species) in stoichiometric balance.

The traditional model of subsurface respiration assumes successive zones of reduction of O_2 , NO_3^- , oxidized manganese (Mn[IV]), oxidized iron (Fe[III]), SO_4^{2-} , and carbon dioxide (CO_2) with increasing distance from the oxic surface world. In marine sediment, this sequence is vertical, with increasing depth below seafloor^{40,41} (Box 1). In aquifers with active fluid flow, the sequence depends on distance from the location where the fluid enters the aquifer from the surface⁴², e.g., the location where seawater enters the subsurface igneous basement.

Most metabolic activities known to occur in subsurface ecosystems were first discovered in surface or near-surface ecosystems. However, a few were first discovered in subsurface sediment, including anaerobic oxidation of methane⁴³, sulfate-reducing ammonium oxidation⁴⁴, and microbial production of ethane and propane⁴⁵.

The specific taxa responsible for individual metabolic activities are not yet known for most subsurface environments⁴⁶. The taxa responsible for specific activities may vary considerably in space and time; a recent metagenomic study of subsurface planktonic

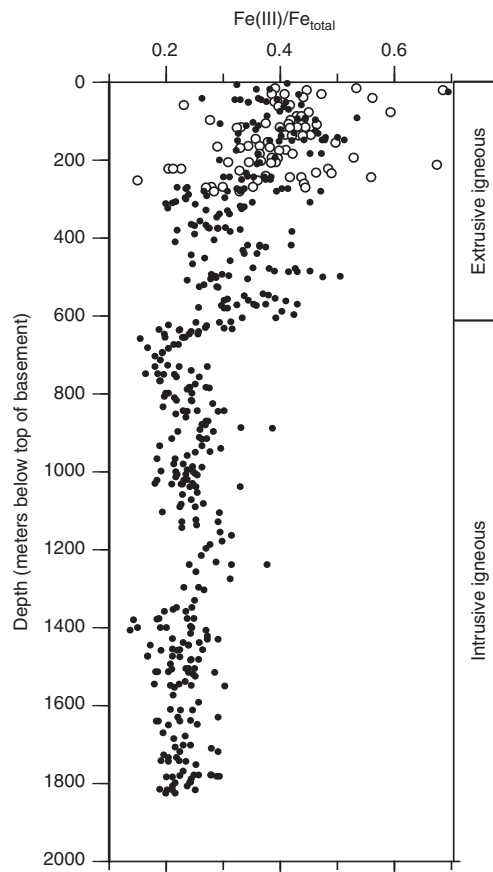


Fig. 3 Profile of Fe oxidation ratio $[Fe(III)/Fe_{total}]$ as function of basement depth. $Fe_{total} = Fe(III) + Fe(II)$. Higher ratios of $Fe(III)/Fe_{total}$ show that a larger fraction of the total Fe is oxidized. Filled circles mark data from DSDP Hole 504B. Open circles mark data from ODP Hole 896 A. All data from Alt et al.²⁰. Figure modified from Alt et al.²⁰

communities in a cold oxic basalt aquifer found a high degree of metabolic functional redundancy over two years of sample collection, despite large shifts in community composition³⁷.

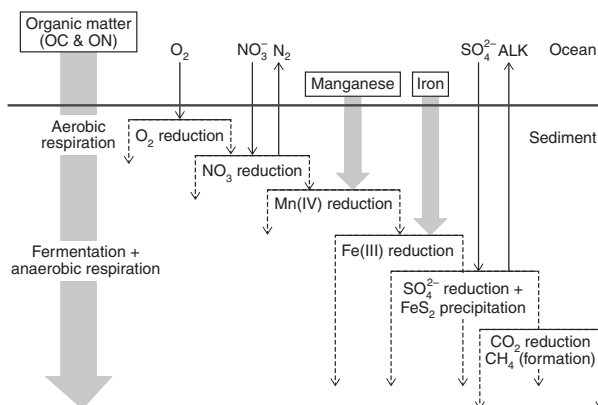
Global consequences of subsurface biological activities. Subsurface microbial activity has at least five major consequences for global biogeochemical cycles (Fig. 4). First, it plays an important role in the oxidation-reduction (redox) evolution of Earth's surface and near-surface environments⁴⁷. Burial of organic matter is the principal pathway for removing reduced material from the surface world and subsurface microbial activity limits the rate of organic burial. In other words, subsurface microbial activity is the final throttle on the primary driver of Earth's surface oxidation. Second, pyrite (FeS_2) produced as a result of microbial SO_4^{2-} reduction in marine sediment is the principal sink for sulfur from the world ocean⁴⁸. Third, this microbially driven pyrite production is a principal source of alkalinity to the world ocean¹¹. These consequences of pyrite precipitation are significant for two reasons: sulfate and bicarbonate (the principal contributor to alkalinity) are the second and third most abundant anions in seawater (after chloride)⁴⁹, and alkalinity influences the distribution of CO_2 between the atmosphere and ocean by determining the speciation of dissolved inorganic carbon. Fourth, subsurface NO_3^- reduction decreases the amount of biologically fixed nitrogen available for marine biomass production (which is often N-limited)⁵⁰. Fifth, subsurface microbial activities play a

Box 1 | Co-occurrence of terminal electron-accepting processes

The standard model of redox zonation in marine sediment assumes successive zones of reduction of O_2 , NO_3^- , oxidized manganese [Mn(IV)], oxidized iron [Fe(III)], SO_4^{2-} and CO_2 with increasing sediment depth. These chemicals, and the material they oxidize, enter sediment at the seafloor; solid phases (manganese- and iron-bearing minerals, organic matter) are deposited with sediment, O_2 , NO_3^- and SO_4^{2-} enter in dissolved form, and most dissolved CO_2 is generated in the sediment by organic oxidation.

This succession of redox zones is generally believed to result from thermodynamic competition, in which organisms that use the actively reduced electron acceptor (e.g., O_2) drive electron-donor concentrations too low to be energetically exploited in combination with less competitive electron acceptors (e.g., CO_2)¹¹⁴. The successive redox activities have been described as mutually exclusive, with less competitive electron acceptors unused until the most competitive electron acceptor is exhausted⁴¹. For example, it has been assumed that SO_4^{2-} is not reduced until accessible Fe(III) is exhausted¹¹⁴.

This standard model explains many broad patterns of subseafloor metabolism. It explains the near-seafloor succession of net oxidant consumption in anoxic sediment throughout much of the ocean^{40,41}. It explains the dominance of oxic respiration over almost 40% of the seafloor (Fig. 1), where sediment accumulates very slowly and dissolved O_2 penetrates the sediment to basement¹⁶. It explains reversed sequences of net redox activities where oxic seawater diffuses upward into anoxic sediment from the underlying basaltic aquifer^{16,21,66} and where sulfate-bearing water diffuses upward into sulfate-depleted sediment^{21,115}.



Some patterns of subseafloor respiration modify the standard zonation, but do not necessarily challenge the assumption that the different processes are mutually exclusive. First, discrete zones of net Fe(III) reduction and net Mn(IV) reduction occur deep beneath zones of net SO_4^{2-} reduction in some sediment²¹. These occurrences can be explained by original deposition of much higher oxidized metal concentrations or much lower organic matter concentration in deep metal-reducing zones than in shallower deposits. Second, isotopic data, transcriptomic data and radiotracer data have respectively been interpreted as evidence of NO_2^- oxidation¹¹⁶, NO_3^- reduction²⁵ and SO_4^{2-} reduction¹¹⁷ in sediment deep beneath the last occurrences of measurable O_2 , NO_3^- and SO_4^{2-} . These processes can only occur at these depths if cryptic processes, such as reduction of H_2O_2 from water radiolysis³⁸, sustain in situ production of the necessary electron acceptors (O_2 , NO_3^- , SO_4^{2-}).

A third pattern is consistent with thermodynamic competition, but disproves the assumption that the competing processes are mutually exclusive. As indicated by the dashed arrows in this figure, these processes often co-occur. O_2 reduction and NO_3^- reduction co-occur at low dissolved O_2 concentrations⁶⁵. NO_3^- reduction and Mn(IV) reduction also often co-occur⁶⁵. SO_4^{2-} reduction and methanogenesis commonly co-occur in marine sediment^{11,28,45}, along with Fe(III) reduction²⁸, throughout sequences that span hundreds of meters and were deposited over millions of years. Fe(III) reduction has also been observed in the methanogenic zone⁴² and the sulfate-reducing zone of continental aquifers¹¹⁸.

Studies of SO_4^{2-} reduction, Fe(III) reduction and methanogenesis indicate that where these processes co-occur, they may compete for electron donors but operate at the same in situ energy of reaction²⁸. This in situ energy closely matches the minimum reaction affinity, A ($A = -\Delta G$ of the reaction)¹¹⁹, believed necessary for an organism to sustain an energy-conserving reaction^{77,108,109}. Estimates of minimum affinities of energy-conserving anaerobic reactions are generally in the range of 2–5 kJ per mole of electrons transported^{77,109}. Affinities in this range have been observed for multiple reactions in both shallow^{44,77} and deep^{28,44} marine sedimentary ecosystems.

Co-occurrence of these competing reactions may aid the organisms that rely on them, by removing reaction products and/or creating reactants. Such removal and/or creation may amplify rates of community activity by returning affinities of multiple reactions to the minimum values required to harvest the reaction energy. For example, co-precipitation of dissolved Fe(II) and dissolved sulfide increases affinities of both Fe(III) reduction and SO_4^{2-} reduction²⁸. Oxidation of methane (CH_4) by SO_4^{2-} reduction or Fe(III) reduction increases the affinity of methanogenic reactions, enabling methanogens to generate more CH_4 that can in turn fuel the sulfate-reducing and Fe(III)-reducing reactions^{28,109,118}.

In summary, as each successive electron-accepting process is initiated, it may hold electron donor concentrations too low to be energetically exploited in combination with other electron acceptors¹¹⁴. However, this competitive exclusion holds only until the competing reactions yield minimum harvestable affinities of reaction. At least for Fe(III) reduction, SO_4^{2-} reduction and methanogenesis, concentrations of reactants (including electron donors) and products yield equivalent affinities of reaction and sustain mutually competing processes deep into subseafloor sediment²⁸.

significant role in creating and/or destroying resources of economic interest, including marine deposits of hydrocarbons⁵¹, phosphate⁵², dolomite^{53,54}, and barite⁵⁵.

Impact of subseafloor activity on the global redox budget.

Oxidation-reduction (redox) reactions transfer electrons from one chemical to another. This transfer constitutes one of the most significant processes on Earth's surface. The primary driver of

redox activity on Earth's surface is oxygenic photosynthesis, which converts water and carbon dioxide into oxidized and reduced compounds (O_2 and organic matter, respectively)¹³. Organic-fueled respiration reverses this process by oxidizing the organic matter.

Over Earth history, the ocean and atmosphere have been progressively oxidized by continuous burial of reduced biological products (principally organic matter and pyrite)¹³. This burial results from the failure of subsurface microbes to oxidize all of the

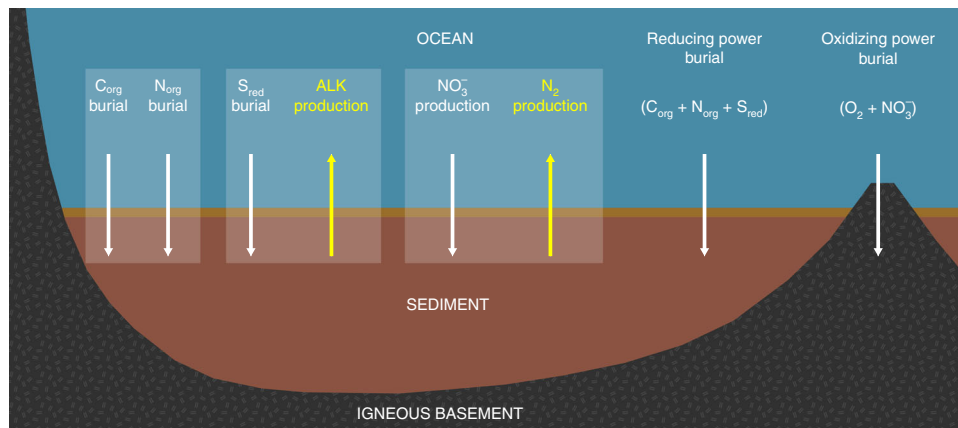


Fig. 4 Major net chemical fluxes due to microbial activities in subseafloor environments. Subseafloor microbial activities control burial fluxes of organic carbon (C_{org}), organic nitrogen (N_{org}), and reduced sulfur (S_{red}) (typically buried as iron sulfide), as well as production fluxes of alkalinity (ALK) and N₂. In doing so, they control the rate at which reducing power is buried. Microbes in igneous basement contribute to burial of oxidizing power (via reduction of O₂ and NO₃⁻)

Table 1 Major net chemical fluxes due to microbial activities in subseafloor environments. Organic carbon burial flux estimates from Sarmiento and Gruber³⁵ and Dunne et al.³⁷. Estimates of NO₃⁻ flux to sediment and N₂ flux from sediment from Gruber⁵⁰. All other fluxes calculated as described in the text. As described in the text, the extent to which microbial activities are responsible for the net oxidizing flux into the igneous basement is not yet known

Process	Net flux into sediment	Net flux out of sediment	Net flux into igneous basement
Organic C burial	1.6–6.5 × 10 ¹³ mol C yr ⁻¹		
Organic N burial	2.4–9.8 × 10 ¹² mol N yr ⁻¹		
Reduced S burial (FeS ₂ precipitation)	2–9 × 10 ¹² mol S yr ⁻¹		
Reducing power burial (C _{org} + N _{org} + S _{red})	1–4 × 10 ¹⁴ mol electron equivalents yr ⁻¹		
Oxidizing power burial (O ₂ & NO ₃ ⁻ reduction)			2.5 ± 1.3 × 10 ¹² mol electron equivalents yr ⁻¹ ?
Alkalinity production from FeS ₂ precipitation		4–18 × 10 ¹² mol alkalinity equivalents yr ⁻¹	
NO ₃ ⁻ reduction	3.6 ± 1.2 × 10 ¹¹ mol N yr ⁻¹		
N ₂ production		3.6 ± 1.2 × 10 ¹¹ mol N yr ⁻¹	

organic matter within sediment and from the microbially mediated transfer of reducing power from organic matter to pyrite. Major manifestations of this long-term oxidation include the precipitation of banded iron oxide deposits during the Archean and early Paleoproterozoic⁵⁶ and the appearance of abundant free O₂ in the ocean and atmosphere⁵⁷. Consequences of this long-term oxidation include Earth’s astonishing diversity of oxygen-reliant organisms⁵⁸, metabolites⁵⁹, and oxidized minerals⁶⁰.

The rate of organic carbon production (net primary production) via photosynthesis is ~4.5 × 10¹⁵ moles C yr⁻¹ in the ocean⁶¹ and ~4.7 × 10¹⁵ moles C yr⁻¹ on land⁶². Organic carbon flux to the seafloor is ~2 × 10¹⁴ moles C yr⁻¹^{61,63}. Assuming a typical marine organic ratio of nitrogen to carbon in the seafloor organic flux (0.15)⁶⁴, organic nitrogen flux to the seafloor is ~0.3 × 10¹⁴ moles N yr⁻¹. Most of the organic-matter flux is ultimately oxidized, sustaining life at the seafloor and within the sediment. However, a significant fraction of the organic flux to the seafloor is permanently buried, rather than respired; the net organic C burial rate in marine sediment is in the range of 0.2 × 10¹⁴ moles C yr⁻¹⁶¹ to 0.7 × 10¹⁴ moles C yr⁻¹⁶³ (Table 1). Most of the flux to the seafloor (70–85%) and the long-term burial (~90%) occurs in coast and shelf environments, in water depths shallower than 200 meters^{61,63}.

By oxidizing organic matter in marine sediment, microbial communities reduce the mean oxidation state of the ocean and atmosphere. From a global redox perspective, this effect is a subseafloor manifestation of the same processes that consume organic matter in the surface world. Net microbial respiration in marine sediment generally consumes both oxidants (electron acceptors) and reductants (electron donors) that originated in the surface photosynthetic world. The principal net oxidants include dissolved species (O₂, NO₃⁻, SO₄²⁻) that diffuse into sediment from the overlying ocean, and solid-phase oxidized metals (e.g., Fe[III] and Mn[IV] in minerals). The principal net reductant is buried organic matter. The principal products of organic-fueled respiration in marine sediment are dissolved inorganic carbon (DIC = HCO₃⁻ + CO₃²⁻ + dissolved CO₂) and dissolved nitrogen species. This DIC generally has one of three fates: some returns to the ocean via diffusion and/or advection as DIC, some is incorporated into carbonate minerals (e.g., CaCO₃) and remains buried, and some is buried as DIC where sediment accumulates faster than chemicals can diffusively return to the ocean. Nitrogen in buried organic matter is released by organic degradation as ammonium (NH₄⁺) and amines⁵⁰. Much of this reduced nitrogen is oxidized to NO₃⁻ and returns to the ocean. Some of this NO₃⁻ is transformed to N₂ (denitrified) during its migration to the ocean. Some of the reduced nitrogen is buried as

dissolved NH_4^+ , incorporated into mineral phases, or transformed to N_2 by anaerobic processes⁴⁴.

For this review, we quantify sedimentary redox fluxes in terms of the number of electrons transferred during reduction from the chemical species stable in contact with Earth's oxygenated atmosphere (e.g., CO_2 , SO_4^{2-} , NO_3^-) to the reduced chemical species that persist in subsurface sediment (e.g., organic matter, FeS_2) (Methods). We similarly quantify basement redox fluxes in terms of the electron numbers required to oxidize the reduced chemicals in basalt. Previous studies have presented redox fluxes in terms of O_2 equivalents⁴⁷ or H_2 equivalents,¹³ one O_2 equivalent corresponds to four electron equivalents and one H_2 equivalent corresponds to two electron equivalents.

The total electron-equivalent burial rate in marine sediment, including reduced C, N and S, is 1×10^{14} to 4×10^{14} moles $\text{e}^- \text{yr}^{-1}$ (Table 1). The marine sedimentary organic carbon burial rate of 1.6×10^{13} to 6.5×10^{13} moles C yr^{-1} ^{61,63} equals 6.4×10^{13} to 2.6×10^{14} moles $\text{e}^- \text{yr}^{-1}$. Assuming an N/C ratio equal to typical marine organic matter (0.15)⁶⁴, the marine sedimentary organic nitrogen burial rate is 2.4×10^{12} to 9.8×10^{12} moles N yr^{-1} (Table 1). Electron-equivalent burial as organic nitrogen (1.9×10^{13} to 7.8×10^{13} moles $\text{e}^- \text{yr}^{-1}$) is $\sim 1/3$ the rate of electron-equivalent burial as organic carbon.

Marine sedimentary communities also modulate redox pathways by transferring electrons from one buried chemical species to another, most notably by transferring electrons from organic matter to iron and sulfur, leading to FeS_2 formation. In this case, reducing equivalents (electron equivalents) that were originally buried with organic matter continue to be buried with the sulfur and iron to which they were transferred. This transfer of electrons is significant. Given an average burial ratio of organic carbon to reduced sulfur in marine sediment (7.5 mole C/mole S)⁶⁵ and the organic burial rates mentioned above, the rate of reduced sulfur burial, principally as FeS_2 , is 2×10^{12} to 9×10^{12} moles S yr^{-1} (Table 1). The burial rate of electron equivalents as reduced sulfur (1.4×10^{13} to 6.3×10^{13} moles $\text{e}^- \text{yr}^{-1}$) is approximately 1/4 the rate of electron-equivalent burial as organic carbon and slightly lower than the rate of electron-equivalent burial as organic nitrogen.

Oxidation of the fractured igneous basement that underlies the sediment also plays a role in global redox cycling, by reducing the oxidation state of the ocean and atmosphere⁴⁷. As seawater hydrothermally circulates through this aquifer, electron acceptors from the ocean, principally O_2 and NO_3^- , oxidize reduced elements, principally iron and sulfur, in igneous minerals¹⁸. This circulation introduces electron acceptors to the upper crust throughout much of the ocean; dissolved O_2 and NO_3^- is present in Eocene and Miocene basalt of the eastern Pacific²¹, Pleistocene to Cretaceous basalt of the central South Pacific¹⁶, and Miocene basalt of the North Atlantic⁶⁶. The resulting oxidation of $1.7 \pm 1.2 \times 10^{12}$ moles Fe yr^{-1} and $1.1 \pm 0.7 \times 10^{11}$ moles S yr^{-1} ¹⁸ reduces the ocean and atmosphere by $2.5 \pm 1.3 \times 10^{12}$ moles $\text{e}^- \text{yr}^{-1}$ (Table 1). The extent to which microbial respiration drives this oxidation is unknown, because dissolved O_2 and NO_3^- abiologically oxidize reduced iron and sulfur⁶⁷.

Multiple lines of evidence suggest that microbes harvest at least some of the energy from the mineral-oxidation reactions in the igneous basement. Microbial communities are routinely sampled from the basement aquifer^{3,36}, members of these communities readily colonize fresh mineral surfaces^{68,69}, and chemical data indicate that microbes play a role in late stages of rock alteration within the aquifer (e.g., SO_4^{2-} reduction, methanogenesis)^{4,5}. However, the extent to which subsurface communities utilize the energy from these reactions is unknown. More importantly for this review, the net effect of that harvest on the global redox cycle

is also unknown. For example, it is not yet clear if microbial communities enhance the total rate of basement oxidation by increasing the extent to which these reactions penetrate into the rock.

Impact on the global sulfur cycle. As the primary sink of sulfur from the ocean⁴⁸ and a major source of alkalinity to the ocean¹¹, SO_4^{2-} reduction coupled to FeS_2 precipitation in marine sediment directly affects ocean chemistry and indirectly affects atmospheric chemistry and climate. Sulfate is the dominant electron acceptor in the anoxic sediment that blankets $\sim 60\%$ of the seafloor. However, only a fraction of the sulfur reduced globally in marine sediment is precipitated as FeS_2 . Sulfur is reduced at the shallowest depths and highest rates in coastal environments, where up to 95% of the resulting sulfide diffuses upward and is re-oxidized⁷⁰. In open-ocean environments, such as the equatorial Pacific, SO_4^{2-} is reduced at greater sediment depths and iron concentration is great enough that $\sim 100\%$ of the reduced sulfur precipitates as FeS_2 ⁷¹.

The natural (pre-anthropogenic) flux of sulfur to the ocean is almost entirely via rivers. A recent estimate of this flux is $\sim 2 \times 10^{12}$ moles S yr^{-1} ⁴⁸. This estimate ignores rapid cycling of sulfur between the ocean and the immediately overlying atmosphere. It also ignores rapid microbial cycling of sulfur reduction and re-oxidation in shallow marine sediment and the water column of oxygen-minimum zones. Again ignoring these rapid cycles, the flux of sulfur from the ocean is almost entirely via metal sulfide precipitation (primarily FeS_2 in marine sediment)^{13,48}. As discussed above, we estimate the rate of reduced sulfur burial in marine sediment to be 2×10^{12} to 9×10^{12} moles S yr^{-1} (Table 1).

Impact on alkalinity and atmospheric CO_2 . Precipitation of metal sulfide following SO_4^{2-} reduction removes the anionic charge of SO_4^{2-} from the ocean. This charge is balanced by production of alkalinity¹¹ (alkalinity is equal to the sum of positive charge equivalents minus the equivalents of negative charge from the conjugate bases of strong acids [Cl^- and SO_4^{2-}])⁴⁹. Consequently, precipitation in marine sediment of 2×10^{12} to 9×10^{12} moles reduced S yr^{-1} generates 4×10^{12} to 1.8×10^{13} moles of alkalinity equivalent yr^{-1} (Table 1). Given these estimates and a riverine primary alkalinity flux to the ocean of 1.3×10^{13} mole equivalents yr^{-1} ⁷², microbially induced precipitation of sedimentary FeS_2 generates 24–58% of the annual primary alkalinity flux to the ocean. CO_2 partial pressure (p_{CO_2}) is highly sensitive to the value of alkalinity; for present-day ocean chemistry, a 25% increase in alkalinity will decrease atmospheric p_{CO_2} by more than an order of magnitude (Methods).

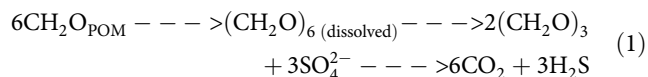
Impact on the global nitrogen cycle. Ongoing burial of organic nitrogen is the primary sink of nitrogen from the atmosphere and ocean. Furthermore, microbial NO_3^- reduction (denitrification) linked to organic matter oxidation in marine sediment is the principal sink of fixed nitrogen from the ocean; the rate of sedimentary NO_3^- reduction is about a factor of two greater than the rate of denitrification in the water column and an order of magnitude larger than the rate of organic nitrogen burial⁵⁰. In the absence of sedimentary denitrification, most marine ecosystems would not be nitrogen-limited. Most of this denitrification occurs in coast and shelf sediment, where the flux of organic matter to the seafloor is highest.

Impact on geological resources. Subseafloor microbial activities also play significant roles in creating and destroying resources of economic interest. The importance of subsurface microbial

activities is most fully delineated for destruction of subseafloor hydrocarbon resources⁵¹. More than 90% of the methane produced in marine sediment is consumed by anaerobic communities within the sediment⁷³. Biodegradation is also extensive in relatively cool (50 °C) marine oil reservoirs, which have typically lost up to ~50% of their mass of C₆₊ hydrocarbons⁵¹. Biodegradation decreases greatly as a function of reservoir temperature. Evidence of oil biodegradation is generally absent from reservoirs warmer than 80 °C, suggesting that the thermal limit to life in the reservoirs is close to that temperature⁵¹. Although microbial roles are less thoroughly studied for production and destruction of other economic resources, rates and subsurface locations of organic oxidation, sulfate reduction and methane production are known to play central roles in precipitating sedimentary deposits of phosphate⁵², barite⁵⁵, dolomite^{53,54}, and gas hydrates. Microbial activities may also play central roles in formation of marine metal deposits, including hydrothermal sulfides⁷⁴.

The limits of subseafloor activity. Since active subseafloor communities are present throughout the world ocean, a paramount biogeochemical mystery has been the failure of those communities to completely consume the electron donors present in subseafloor environments. Even in oxic marine sediment, traces of organic matter may survive for 100 Myrs or more¹⁶. Reduced iron and reduced sulfur persist in subseafloor basalt for more than 100 Myrs¹⁸. This failure plays a significant role in the redox evolution of Earth's atmosphere and ocean, because, as described above, sequestration of organic matter in marine sediment is a principal sink for reducing power from the surface world. Furthermore, failure of microbial communities to oxidize all of the iron and sulfur in the subseafloor igneous aquifer leaves oxidizing power in the ocean that might have otherwise been lost to mineral oxidation. The failure to consume all of the buried organic matter also decreases the influence of subseafloor respiration on global cycles of sulfur, nitrogen and alkalinity. The persistence of organic matter in marine sediment is also crucial for thermogenic formation of major hydrocarbon resources, because oil and gas cannot form in the absence of their feedstock.

Not all sedimentary organic matter is consumed. Organic oxidation rate is generally highest at the seafloor and decreases with sediment depth, declining rapidly near the seafloor and increasingly slowly with greater distance from the seafloor. This relationship is typically modeled as a power-law function^{17,75,76}. The basic reaction series can be simplified as follows:



Standard models of organic persistence in marine sediment assume that the first step is the rate-limiting step⁷⁵. However, if organisms are operating at their minimum harvestable reaction affinity⁷⁷, catabolic reactions cannot proceed faster than reactants appear or reaction products disappear at the reaction location⁷⁸. In this case, the rate-limiting step may occur later in the reaction series, such as the final respiration step of the above sequence, which will be limited by the rates at which SO₄²⁻ is introduced and the rate(s) at which CO₂ and H₂S are removed (Box 2).

This dependence of organic oxidation rate on chemical fluxes and minimum reaction affinity will naturally lead to the typical depth-dependence of organic oxidation rate (Box 2). Because the time required for chemical diffusion is proportional to the square of diffusive distance⁷⁹, where advection is insignificant (below the depth of bio-irrigation), organic oxidation rate must decline exponentially with distance from sources of catabolic reactants and sinks of catabolic products (Box 2). Where electron acceptors

and catabolic products respectively diffuse from and to the ocean above, the rate of organic oxidation will decline exponentially with depth beneath the seafloor.

Most quantitative models of the decline in bulk organic oxidation rate with sediment depth assume that organic persistence results from organic molecular structure, with selective preservation of the least reactive (most carbon-rich) compounds^{75,76}. These models are variations on Berner's 1964 G Model, which assumed organic oxidation rate to be proportional to organic matter concentration⁷⁶. More recent models assume that bulk organic oxidation rate declines with sediment depth and age because increasingly recalcitrant pools of organic matter are successively depleted¹⁷. This assumption is consistent with laboratory experiments that show sequential utilization of different sedimentary organic carbon pools by aerobic heterotrophs⁸⁰. Despite this consistency, reliance on relative degradability to explain organic oxidation rates is problematic for the following reasons. First, the molecular composition of these organic pools is never identified by studies that assume them to model organic oxidation rates^{17,76}. Second, the degradability of an organic-matter pool, such as kerogen (the fraction of organic matter insoluble to organic solvents) in deeply buried sediment, is not inherent to the organic molecules that compose that pool, but depends on the environment in which the organic pool is present⁸¹. For example, 365-million-year-old organic matter is quickly degraded by microbes when exposed by erosion⁸². Third, preferential degradation or persistence of different classes of organic compounds may be better considered as a function of community metabolic capabilities than as an intrinsic property of organic molecules⁸³. Fourth, preferential persistence of the most carbon-rich compounds is difficult to reconcile with preservation of relatively low C/N ratios for tens of Myrs^{84,85}, and with subseafloor respiration of C/N ratios close to the average marine (Redfield) value for tens of Myrs^{16,29,86}.

Other studies have proposed that organic matter persists because it is adsorbed to mineral grains^{85,87,88}. This hypothesis is consistent with a generally close association between high bulk organic concentrations and abundance of fine-grained minerals⁶⁵. However, reliance on organic adsorption to minerals as the primary explanation of organic persistence in marine sediment is difficult to sustain for the following reasons. First, it is difficult to reconcile the molecular integrity of some compounds, such as certain fatty acids and pigments, with the solubilization that must precede adsorption⁸⁹. Second, discontinuous distribution of organic matter renders binding to mineral grains an insufficient explanation of organic persistence in continental-margin sediment^{65,90}. Third, much of the adsorption to minerals is easily reversed and ultimately cannot preserve organic matter⁹¹.

These different explanations have fundamentally different implications for the relationship between organic oxidation rates and organic-matter persistence in deep old sediment. To the extent that organic oxidation rate depends on minimum reaction affinity and diffusion rates of dissolved catabolic reactants and products (Box 2), organic matter can persist simply because oxidation rate declines with sediment depth. In contrast, selective-preservation hypotheses assume that organic oxidation rate declines because residual organic molecules are chemically recalcitrant. Finally, the mineral adsorption hypothesis could be used to predict that organic oxidation rate declines because residual organic matter is strongly adsorbed to minerals.

Demonstration of increased organic recalcitrance or increased mineral adsorption with sediment age is necessary to respectively support the hypotheses that organic recalcitrance or mineral adsorption drives the decrease in organic oxidation rate with increasing sediment depth and age. However, neither test is sufficient to prove either hypothesis, because organic recalcitrance

Box 2 | Dependence of organic oxidation rate on diffusion timescale

If the affinity of a catabolic reaction drops below the minimum value necessary to sustain biological energy conservation (Box 1), the energy of reaction is not biologically harvestable until the affinity of the reaction rises again. In short, the rate of catabolic activity is limited by the flux of bioavailable energy⁷⁸. As the reaction proceeds, its affinity decreases. When it drops below the minimum value, energy is no longer conserved and the reaction stops until more reactant is introduced or reaction product is removed.

This relationship between the affinity of a reaction and the rate of that reaction is exemplified by chemostats, in which growth rate depends on the rate that reactants are added and products are removed. However, in a chemostat, reactants (e.g., O_2 , NO_3^- , SO_4^{2-}) are typically added by fluid inflow and reaction products [e.g., DIC] are removed by fluid outflow. In contrast, in most marine sediment, catabolic reactants are added and catabolic products are removed via diffusion. Because the timescale of diffusion is proportional to diffusive distance squared⁷⁹, the rates of reactant introduction and product removal via diffusion decrease strongly with distance to the reactant source and distance to the product sink. In effect, increasing sediment thickness drives subsurface ecosystems toward being closed systems⁴⁰.

In other words, the rate of catabolic activity is expected to decrease with distance from where a reactant is introduced or a product is lost, due to the decreasing rate of diffusive transport, even if the lability and concentration of organic matter are constant throughout the sediment column (Methods). The effect of diffusive distance is small for reactants produced in situ³⁸, such as radiolytic H_2 , and products removed in situ, such as sulfide precipitated in FeS_2 at the location of sulfide production. However, this effect can be significant for reactants and products that diffuse to or from elsewhere in the sediment column (e.g., for O_2 , NO_3^- or SO_4^{2-} that diffuses into the sediment from the overlying ocean, and for DIC that diffuses from the sediment into the ocean).

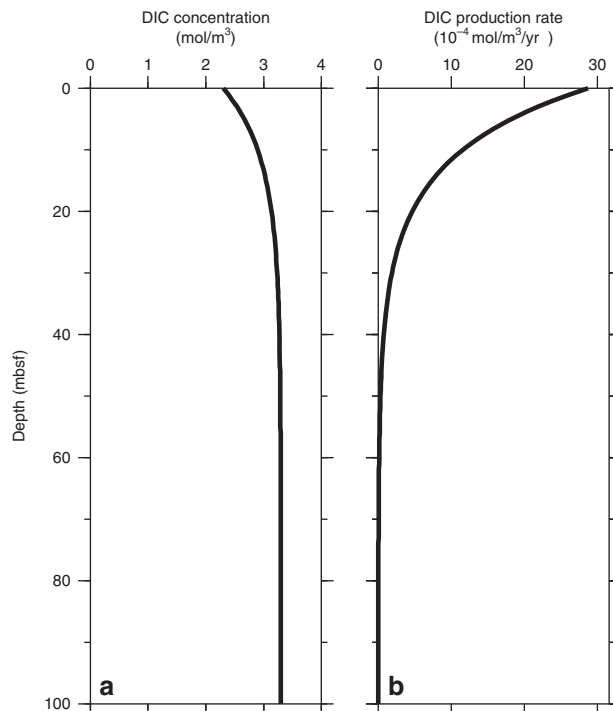
We illustrate this effect with DIC production by sulfate-reducing oxidation of a carbohydrate ($CH_2O + 0.5 SO_4^{2-} \rightarrow HCO_3^- + 0.5 HS^-$). We focus on HCO_3^- because DIC is predominantly HCO_3^- in marine sediment. For simplicity, this example assumes that concentrations of HS^- , CH_2O and SO_4^{2-} are constant or proportionally change to a much lesser extent than HCO_3^- . Given this assumption and reaction affinity at the minimum biologically harvestable value, reaction rate directly depends on the net rate of DIC diffusion at each depth. Expansion of this model to include catabolic reactants, additional reaction products and/or additional reactions (e.g., organic solubilization and fermentation) would complicate the model, but lead to a similar result.

In this model, the HCO_3^- production rate at distance z from the top of a sediment column is given by

$$P(z) = P_{\max}(1 - c(z)/c_{A-\min}) \quad (2)$$

where P_{\max} is the maximum HCO_3^- production rate (which occurs at the top of the sediment column), $c(z)$ is the HCO_3^- concentration at depth z , and $c_{A-\min}$ is the HCO_3^- concentration above which A drops below A_{\min} and energy-yielding HCO_3^- production stops. Balancing diffusive transport with reaction rate parameterized in this way leads to the expectation that catabolic reaction rate decreases exponentially with sediment depth.

This relationship between catabolic rate and diffusive distance is consistent with the generally observed strong and initially rapid decline in organic oxidation rate with sediment depth¹⁷. It is also consistent with the generally strong correlation between organic burial efficiency and sedimentation rate^{65,75}. In the extreme case of fast-accumulating organic-rich sediment, sedimentary communities are buried faster than reactants (such as O_2 , NO_3^- and SO_4^{2-} from the overlying ocean) can diffuse to them and faster than terminal reaction products (such as DIC and CH_4) can diffuse to a sink (such as the anaerobic methane-oxidizing zone or the seafloor). In this system, abundant and compositionally diverse organic matter may persist in deep sediment because reaction rates are too low to consume it.



and/or mineral adsorption might increase with sediment age even if they do not drive the decrease in organic oxidation rate with sediment depth and age.

Persistence of electron donors in subsurface sediment is not limited to solid-phase organic matter. For example, the turnover times of dissolved fatty acids in sulfate-reducing subsurface

sedimentary ecosystems ranges from approximately tens to hundreds of years (Methods). These relatively long turnover times of dissolved electron donors are not explainable by chemical recalcitrance or adsorption to minerals. However, they are a natural consequence of microbial thermodynamics coupled to subsurface timescales of chemical diffusion (Box 2).

The causal relationship between organic oxidation rates and organic-matter persistence may differ from one marine sedimentary environment to another. Diffusion of chemical species may limit organic oxidation rates in fast-accumulating anoxic sediment, where organic oxidation reactions operate at minimum harvestable affinities of reaction. However, in sediment where electron acceptors are abundant and reaction products are scarce, organic persistence may result from mineral shielding or molecular inaccessibility of the organic matter. Such circumstances might apply in the slowly accumulating organic-poor oxic sediment that blankets much of the abyssal ocean^{16,85}.

The igneous seafloor is not fully oxidized. The factors that limit oxidation rates in the igneous seafloor are rarely addressed explicitly. The permeability of un-fractured basalt is extremely low and rock alteration is closely associated with fractured surfaces⁹². Given these points, persistence of reduced iron and sulfur in seafloor basalt can most simply be ascribed to physical inaccessibility of the reduced elements within the un-fractured rock. This ascription is a variation on the diffusive-timescale explanation that we present for sedimentary organic oxidation above and in Box 2; however, in the igneous basement, permeability is so low that chemical diffusion of electron acceptors into un-fractured rock is extremely slow, even for sub-millimeter distances.

The persistence of dissolved organic matter (DOM) in the igneous aquifer is more enigmatic. DOM enters the aquifer with water from the overlying ocean⁶. Because DOM is in the water, not the rock, it is in contact with dissolved electron acceptors. Although some DOM is consumed within the aquifer, DOM is present along the entire flow path. In the cool oxygenated aquifer of North Pond (North Atlantic), DOM has radiocarbon model ages of several thousand years⁶. These model ages are significantly older than the residence time of water in the aquifer or the residence time of deep water in the North Atlantic, suggesting ongoing supply of aged organic matter to the deep ocean and the aquifer.

Microbial activities and the seafloor limit to life. The preceding paragraphs and Box 2 focus on limits to seafloor activity in environments where organisms are present and metabolically active. In seafloor environments, fluxes of bioavailable energy may be too low to maintain community function under physical conditions that differ notably from physical limits to life in other environments. For example, the high-temperature limit to oil and gas bioalteration (80–90 °C)⁵¹ is considerably lower than the high-temperature limit to life in energy-rich and nutrient-rich autoclave conditions (122 °C)⁸. This difference illustrates that the high-temperature limit to life may vary from one environment to another as a function of bioavailable energy flux or nutrients^{9,51}.

Factors other than temperature may also sterilize seafloor systems. More precisely, changes in chemical conditions might sterilize seafloor environments after multi-Myr intervals of selection for previous chemical conditions. For example, the oxic condition of abyssal clay sequences for tens of Myrs may drive obligate anaerobes in the clay to extinction, to be followed by local extinction of aerobes if sedimentation rates increase and dissolved O₂ disappears from the clay.

Future directions. As indicated in the preceding sections, many key issues remain to be resolved. Global rates of seafloor microbial activities and their consequences are only roughly quantified. For example, recent estimates of organic carbon burial in marine sediment differ by ~4 × ^{61,63} and recent estimates

of global SO₄²⁻ reduction rate in marine sediment differ by ~7.5 × ^{93,94}. Our estimates of FeS₂ precipitation rate, alkalinity production rate and organic nitrogen burial rate in marine sediment are based on estimates of organic carbon burial rate and also vary by ~4 ×. This lack of precision is exacerbated by incomplete understanding of microbial processes in the seafloor. For example, the extent to which microbes participate in redox alteration of inorganic phases in seafloor basalt and sediment remains to be determined. More precisely, the extent to which microbes harvest the energies of mineral-altering redox processes that can proceed abiologically is not known. Furthermore, the extent to which microbes actively enhance mineral alteration, e.g., by mining more deeply or more rapidly into minerals and/or rock than done by abiotic alteration, is also unknown.

The factors that limit rates of seafloor catabolic activities are crucial to the operation of Earth's biogeochemical cycles but not fully understood. Consideration of reaction affinities and dissolved chemical transport suggests that diffusion rates of catabolic reactants and products play an important and previously under-recognized role in limiting seafloor catabolic rates and, thereby, sustaining the persistence of electron donors in seafloor environments.

The specific taxa responsible for individual activities are not known for most seafloor environments⁴⁶. The metabolic networks that sustain their communities for millions of years are largely unexplored. The nature and extent of communication between cells in seafloor communities is unexamined. At the most fundamental biological level, the genomic properties and patterns of gene expression that enable lineages of seafloor microbes to survive at extraordinarily low rates of activity for millions of years remain unknown²⁸.

Better quantification of seafloor microbial activity rates and their consequences will require integration and quantitative analysis of data from diverse studies. For example, more accurately quantifying global burial rates of organic carbon, organic nitrogen and sulfide in marine sediment will require synthesis of geochemical data from shallow and deep sediment of coastal environments, continental shelves and the open ocean. And precise quantification of sulfide burial's effect on ocean alkalinity and atmospheric chemistry will require quantification of both sulfide burial and sulfate flux to the ocean.

Deeper understanding of seafloor activities and their consequences will require Earth and life scientists to deliberately integrate techniques from diverse fields (e.g., molecular biology, aqueous geochemistry, sedimentology, petrology and mineralogy) to test key hypotheses. For example, fuller understanding of how dissolved chemical transport and reaction affinities limit rates of seafloor activities – and ultimately control global biogeochemical fluxes – will require integrated study of *in situ* abilities to undertake specific catabolic reactions, *in situ* reaction rates, and *in situ* energies of reaction.

Hypothesis-driven laboratory experiments and direct study of natural communities will both be crucial to advance understanding of the physiological features, metabolic strategies, and genomic properties that enable lineages of seafloor microbes to persist at extraordinarily low rates of activity for millions of years. Laboratory experiments are necessary to elucidate the features and strategies that enable microbes to thrive or survive under specific seafloor conditions, at least on laboratory timescales, and the genes that code for those features and strategies. Direct studies of natural seafloor communities are needed to delineate the conditions in which they live, to characterize microbial interactions in seafloor communities, and to identify features and strategies that enable microbial

lineages and communities to thrive or survive under subseafloor conditions for many millions of years.

With both laboratory experiments and natural-sample studies, a broad range of analytical approaches is crucial to understand the organisms and communities. Genomic studies are necessary to know what capabilities are available. Transcriptomic studies are needed to understand which capabilities are expressed. Biogeochemical studies are required to determine in situ reaction rates, in situ energies of reaction, and consequences of microbial activities. Exacting studies of organic composition and mineral composition are necessary to identify the substrates available to subseafloor organisms and the consequences of microbial activities. Natural-community studies often benefit from explicitly placing them in a temporal context, e.g., by repeatedly sampling a subseafloor flow path over time³⁷, by sampling crust of very different ages, or by treating data from younger samples in the same sediment column as potentially representative of earlier stages in the history of a subseafloor community^{29,95,96} or habitat. Such temporal context is crucial for understanding how subseafloor communities are assembled. It is also critical for understanding how their biogeochemical roles and consequences vary throughout the subseafloor in space and time.

Individual studies need not integrate across many categories of study. Appropriate laboratory experiments can bring great value whether they are tied to specific field sampling programs or not. Similarly, well-posed natural-sample studies can effectively address key problems (e.g., quantification of specific biogeochemical fluxes or identification of globally consistent genomic and/or transcriptomic patterns) without close integration to other categories of natural-sample study or to laboratory experiments. Ultimately, however, each category of study derives greater strength by integration with one or more of the other categories. For example, laboratory studies inform the understanding of data from subseafloor samples, and subseafloor data inform the hypotheses that drive the laboratory experiments. Understanding of natural subseafloor communities and their consequences also benefits from synthesizing results of different approaches to natural samples. For example, biogeochemical results might explain why a specific capability that is present is not expressed, and genomic studies might explain why a reaction that is energetically feasible does not occur.

As shown by these examples, close integration of biological, chemical and physical approaches will ultimately be necessary to further advance understanding of subseafloor life and its biogeochemical consequences. This integration will require both Earth and life scientists to begin thinking of many geological and geochemical features (such as organic recalcitrance and rates of subseafloor redox processes) as ecosystem properties, rather than a priori environmental features.

Methods

Calculation of habitable basement volume. The total volume (rock + water) of submarine igneous basement cooler than 122 °C is 3.0×10^8 km³. We calculated this total volume using the method of Heberling et al.⁹⁷; however, instead of globally averaged theoretical and observed heat flow values⁹⁸ and constant sedimentation rate of 3 m Myr⁻¹, we used global grids of heat flow⁹⁹ and sediment thickness¹⁰⁰ to calculate global maps of depth to the 122 °C isotherm with a grid resolution of 0.1 × 0.1 degrees. We then spatially integrated these depths to calculate a global volume.

Assuming 10% in upper 500 m of basement and a linear decrease in porosity to zero at 1000 m into basement¹⁰¹, habitable pore space in the basement is 2.2×10^7 km³ (about 2% of ocean volume).

Determination of dissolved O₂ and SO₄²⁻ distributions. We used interstitial water concentrations of dissolved O₂ and SO₄²⁻ from ODP and IODP drill sites¹⁰² and a two-step approach to create the global map of electron acceptor distributions in sediment (Fig. 1). The first step was to plot the chemical species as a function of sediment depth and note whether their concentration goes to zero within the

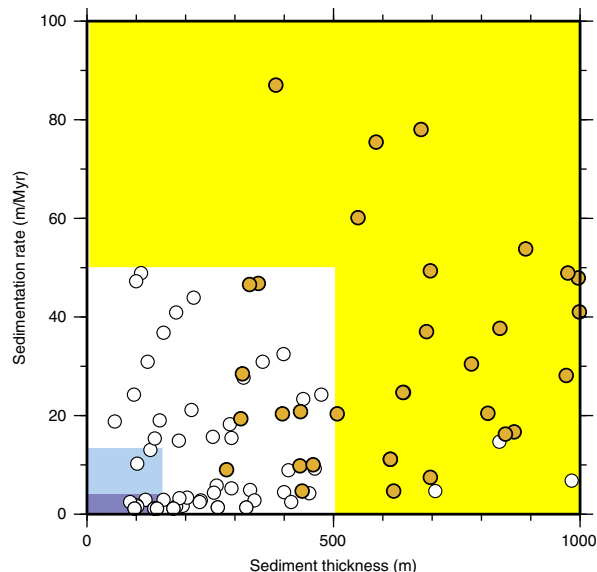


Fig. 5 Plot of sediment thickness and sedimentation rate at ODP and IODP sites. Only sites where dissolved SO₄²⁻ has been measured in sedimentary porewater are shown. Orange dots indicate sites where SO₄²⁻ concentrations go to zero within the upper 500 m of sediment. White dots indicate sites where SO₄²⁻ is present from seafloor to basement. The yellow, dark blue and light blue fields identify the sediment thickness and sedimentation rate boundaries used to generate Fig. 1. The blue fields are based on previous results for dissolved O₂ reported by D'Hondt et al.¹⁶. Dissolved O₂ may or may not be present throughout the sediment at sites marked by white dots in the blue fields; no O₂ measurements were made at these sites. White dots in the yellow areas include sites where flow introduces SO₄²⁻ through rubble or from beneath the seafloor and sites where SO₄²⁻ diffuses upward from underlying brine. Orange dots in the white field generally mark sites where dissolved chemical concentrations are not at diffusive steady state (e.g., because sedimentation rate has been unusually high in the recent geologic past)

sediment or is non-zero all the way to basement. Of 380 ODP and IODP drill sites with SO₄²⁻ data, SO₄²⁻ concentrations go to zero within the sediment at 150 sites, 70 sites had non-zero SO₄²⁻ concentrations from seafloor to basement, and 160 sites were undetermined because the sites were not drilled to basement or SO₄²⁻ measurements were stopped at depths far above basement. The dissolved O₂ results were previously reported in D'Hondt et al. (2015)¹⁶.

The second step identified relationships between the presence and absence of the various chemical species as a function of sedimentation rate and total sediment thickness. This method was previously used for O₂ in sediment;¹⁶ we extended it to include the SO₄²⁻ data (Fig. 5). Our results indicate that SO₄²⁻ goes to zero in the sediment column when sediment thickness exceeds about 500 m or sedimentation rate exceeds 35 m Myr⁻¹. In comparison, dissolved O₂ concentrations go to zero in the sediment where sediment thickness exceeds about 150 m or sedimentation rate exceeds 15 m Myr⁻¹. These 'boundaries' for persistence or absence of SO₄²⁻ to igneous basement were combined with similar boundaries for dissolved O₂ (e.g., D'Hondt et al., 2015) to generate Fig. 1 from global sediment-thickness maps¹⁰⁰ and depth-averaged sedimentation rates. The depth-averaged sedimentation rates were derived from the sediment thickness maps and global maps of ocean basement age¹⁰³.

Reaction-rate calculations. To quantify net rates of O₂ reduction (IODP Site U1370) and SO₄²⁻ reduction (ODP Sites 1226 and 984) from dissolved chemical data (Fig. 2a–c), we used a modified version of the Matlab-based numerical procedures of Wang et al.⁷¹. We modified the approach of Wang et al. by using an Akima spline, instead of a 5-point running mean, in order to generate a best-fit line to the chemical concentration data. We determined standard deviations through use of a Monte Carlo simulation ($n = 50$). For these calculations, diffusivities are from Schulz¹⁰⁴, corrected for in situ temperature at Sites 1226 and U1370 (temperature was assumed constant at Site 984, where in situ temperature was not measured). Porosities and in situ temperature data are from shipboard measurements of the respective drilling expeditions^{105–107} (available at <http://sedis.iodp>).

org). Sedimentation rates are from the shipboard age models generated for each drill site^{105–107}.

Calculation of electron-equivalent burial rates. We calculate electron-equivalent burial rates by multiplying the difference between the dominant oxidation state of the chemical element (C, N or S) at Earth's surface and its oxidation state in marine sediment. The dominant surface-Earth oxidation states for C, N, and S are IV, 0 and VI, respectively. The oxidation states in marine sediment are taken as 0, -III and -I for organic C, organic N and S in FeS₂.

Calculation of alkalinity effect on CO₂ partial pressure. Increasing alkalinity from present ocean values will cause net conversion of dissolved CO₂ to predominantly HCO₃⁻ and to a lesser extent CO₃²⁻ (dissolved CO₂ = H₂CO₃ + CO₂). We calculated the exact change in equilibrium CO₂ partial pressure for a given change in alkalinity using the thermodynamic constants for the aqueous CO₂ system⁴⁹.

Dependence of organic degradation on diffusive distance. Our idealized model of the depth dependence of organic degradation rate assumes that the rate of a catabolic reaction sequence (i.e., production of a sugar monomer from particulate organic matter, followed by fermentation and respiration), occurs at or near steady state at a given sediment depth and that the energy ($-\Delta G$) yielded by each biologically conserved reaction (fermentation or respiration) must equal or exceed the minimum amount that can be biologically conserved ($\Delta G_{\text{minimum}}$)^{77,108,109}. That is, the affinity ($A = -\Delta G$) for each catabolic reaction must equal or exceed the biological minimum affinity (A_{minimum}). This assumption is supported by observations of in situ energies of reactions in marine sediment^{44,77,110,111}. Here, we use SO₄²⁻ reduction as an example. In this approach, the catabolic production rate of DIC (of which HCO₃⁻ is the major species) depends on the HCO₃⁻ concentration, $1 - c/c_{A-\text{min}}$, to keep $A \geq A_{\text{minimum}}$, where $c_{A-\text{min}}$ is the HCO₃⁻ concentration above which A drops below A_{minimum} and the reaction sequence does not proceed. This dependence of rate on metabolite concentrations was previously applied by Boudart (1978)¹¹² to generic reaction sequences and adopted by Jin and Bethke (2009)⁷⁸, and Dale et al. (2008)¹¹³. We extend this approach by explicitly identifying the effect of diffusive distance on reaction rate, via its effect on metabolite concentrations. We choose HCO₃⁻ for this demonstration because, in sulfate-reducing sediment where sulfide is scavenged by iron, HCO₃⁻ exhibits the largest relative change in concentration.

$P(z)$, the production of DIC at depth z is then given by

$$P(z) = P_{\text{max}}(1 - c(z))/c_{A-\text{min}} \quad (2)$$

where $c(z)$ is the HCO₃⁻ concentration at depth z , and P_{max} is the rate when $c = 0$ and the local mass balance is

$$\frac{\partial c(z, t)}{\partial t} = 0 = D \frac{\partial^2 c(z, t)}{\partial z^2} + P(z) \quad (3)$$

$$0 = D \frac{\partial^2 c(z, t)}{\partial z^2} + P_{\text{max}} \left(1 - \frac{c(z)}{c_{A-\text{min}}} \right) \quad (4)$$

where D is the HCO₃⁻ diffusion constant. A solution to Eq. (3) is

$$c(z) = (c(z=0) - c_{A-\text{min}}) * \exp(-P_{\text{max}}/(D * c_{A-\text{min}}) * z) + c_{A-\text{min}}$$

and the depth-dependent metabolic rate is then

$$P(z) = P_{\text{max}} * \exp((-P_{\text{max}}/(Dc_{A-\text{min}})^{0.5} * z))$$

Where P_{max} = DIC production rate when $c_{\text{DIC}} = 0$.

Turnover-time calculations. The turnover times of low-molecular-weight fatty acids are calculated as the concentration of lactate, acetate or formate divided by the rate of SO₄²⁻ reduction corrected for stoichiometry (respectively 1.0, 0.67, and 0.5 times the rate of SO₄²⁻ reduction for acetate, lactate, and formate) at IODP Site 1226, a site where SO₄²⁻ is reduced but not entirely depleted. The different ratios to SO₄²⁻ reduction are used to account for the different oxidation states and numbers of carbon atoms in each molecule, assuming the initial particulate organic carbon (POC) had oxidation state 0. Because we do not know the fraction of total SO₄²⁻ reduction rate that goes to oxidize each of these low-molecular-weight acids, we calculated a potential range of turnover times based on each one separately. At this site, concentrations of these low-molecular-weight fatty acids are all in the range of 1 μM¹¹¹ and the subsurface SO₄²⁻ reduction rate declines from 3×10^{-8} moles liter⁻¹ yr⁻¹ to $\sim 0.2 \times 10^{-8}$ moles liter⁻¹ yr⁻¹ with increasing depth below seafloor⁷¹. Given the relatively constant low-molecular-weight fatty acid concentrations, the decline in SO₄²⁻ reduction rate leads to turnover times increasing from the low tens to low hundreds of years with increasing sediment depth.

Data availability

All data are previously published and accessible as identified in the cited sources.

Received: 21 September 2017 Accepted: 10 July 2019

Published online: 06 August 2019

References

- Kallmeyer, J., Pockalny, R., Adhikari, R. R., Smith, D. C. & D'Hondt, S. Global distribution of microbial abundance and biomass in seafloor sediment. *Proc. Natl Acad. Sci. USA* **109**, 16213–16216 (2012).
- Whitman, W. B., Coleman, D. C. & Wiebe, W. J. Prokaryotes: the unseen majority. *Proc. Natl Acad. Sci. USA* **95**, 6578–6583 (1998).
- Cowen, J. P. et al. Fluids from aging ocean crust that support microbial life. *Science* **299**, 120–123 (2003).
- Alt, J. C. et al. Hydrothermal alteration and microbial sulfate reduction in peridotite and gabbro exposed by detachment faulting at the Mid-Atlantic Ridge, 15°20'N (ODP Leg 209): A sulfur and oxygen isotope study. *Geochem. Geophys. Geosyst.* **8**, 1–22 (2007).
- Lever, M. A. et al. Evidence for microbial carbon and sulfur cycling in deeply buried ridge flank basalt. *Science* **339**, 1305–1308 (2013).
- Shah Walter, S. R. et al. Microbial decomposition of marine dissolved organic matter in cool oceanic crust. *Nat. Geosci.* **11**, 334–339 (2018).
- Fisk, M. R., Giovannoni, S. J. & Thorseth, I. H. Alteration of oceanic volcanic glass: textural evidence of microbial activity. *Science* **281**, 978–980 (1998).
- Takai, K. et al. Cell proliferation at 122 °C and isotopically heavy CH₄ production by a hyperthermophilic methanogen under high-pressure cultivation. *Proc. Natl Acad. Sci. USA* **105**, 10949–10954 (2008).
- LaRowe, D. E., Burwicz, E., Arndt, S., Dale, A. W. & Amend, J. P. Temperature and volume of global marine sediments. *Geology* **45**, 275–278 (2017).
- Eskins, B. W. & Sharman, G. F. *Volumes of the World's Oceans from ETOPO1*. (NOAA National Geophysical Data Center, 2010).
- D'Hondt, S., Rutherford, S. & Spivack, A. J. Metabolic activity of subsurface life in deep-sea sediments. *Science* **295**, 2067–2070 (2002).
- Roy, H. et al. Aerobic microbial respiration in 86-million-year-old deep-sea red clay. *Science* **336**, 922–925 (2012).
- Kasting, J. F. What caused the rise of atmospheric O₂? *Chem. Geol.* **362**, 13–25 (2013).
- Des Marais, D. J. Isotopic evolution of the biogeochemical carbon cycle during the Proterozoic Eon. *Org. Geochem.* **27**, 185–193 (1997).
- Johnson, B. & Goldblatt, C. The nitrogen budget of Earth. *Earth-Sci. Rev.* **148**, 150–173 (2015).
- D'Hondt, S. et al. Presence of oxygen and aerobic communities from sea floor to basement in deep-sea sediments. *Nat. Geosci.* **8**, 299–304 (2015).
- Røy, H. Experimental assessment of community metabolism in the subsurface. in *Microbial Life of the Deep Biosphere* (eds Kallmeyer, J., Wagner, D.) 303–317 (De Gruyter, 2014).
- Bach, W. & Edwards, K. J. Iron and sulfide oxidation within the basaltic ocean crust: Implications for chemolithoautotrophic microbial biomass production. *Geochim. et. Cosmochim. Acta* **67**, 3871–3887 (2003).
- Neira, N. M. et al. Cross-hole tracer experiment reveals rapid fluid flow and low effective porosity in the upper oceanic crust. *Earth Planet. Sci. Lett.* **450**, 355–365 (2016).
- Alt, J. C., Honnorez, J., Laverne, C. & Emmermann, R. Hydrothermal alteration of a 1 km section through the upper oceanic crust, Deep Sea Drilling Project Hole 504B: mineralogy, chemistry and evolution of seawater-basalt interactions. *J. Geophys. Res.* **91**, 10309 (1986).
- D'Hondt, S. et al. Distributions of microbial activities in deep seafloor sediments. *Science* **306**, 2216–2221 (2004).
- Inagaki, F. et al. Biogeographical distribution and diversity of microbes in methane hydrate-bearing deep marine sediments on the Pacific Ocean Margin. *Proc. Natl Acad. Sci. USA* **103**, 2815–2820 (2006).
- Nunoura, T. et al. Variance and potential niche separation of microbial communities in seafloor sediments off Shimokita Peninsula, Japan. *Environ. Microbiol.* **18**, 1889–1906 (2016).
- Ivarsson, M., Bengtson, S. & Neubeck, A. The igneous oceanic crust – Earth's largest fungal habitat? *Fungal. Ecology* **20**, 249–255 (2016).
- Orsi, W. D., Edgcomb, V. P., Christman, G. D. & Biddle, J. F. Gene expression in the deep biosphere. *Nature* **499**, 205–208 (2013).
- Engelhardt, T., Kallmeyer, J., Cypionka, H. & Engelen, B. High virus-to-cell ratios indicate ongoing production of viruses in deep subsurface sediments. *ISME J.* **8**, 1503–1509 (2014).
- Nigro, O. D. et al. Viruses in the Oceanic Basement. *MBio* **8**, 1–15 (2017).
- D'Hondt, S., Wang, G. & Spivack, A. The underground economy (Energetic Constraints of Subseafloor Life). in *Earth and life processes discovered from seafloor environments: A decade of science achieved by the Integrated Ocean Drilling Program (IODP)* 127–148 (Elsevier, 2014).

29. Walsh, E. A. et al. Relationship of bacterial richness to organic degradation rate and sediment age in subseafloor sediment. *Appl. Environ. Microbiol.* **82**, 4994–4999 (2016).
30. Biddle, J. F., White, J. R., Teske, A. P. & House, C. H. Metagenomics of the subsurface Brazos-Trinity Basin (IODP site 1320): Comparison with other sediment and pyrosequenced metagenomes. *ISME J.* **5**, 1038–1047 (2011).
31. Breuker, A., Stadler, S. & Schippers, A. Microbial community analysis of deeply buried marine sediments of the New Jersey shallow shelf (IODP Expedition 313). *FEMS Microbiol. Ecol.* **85**, 578–592 (2013).
32. Brandt, L. D. & House, C. H. Marine subsurface microbial community shifts across a hydrothermal gradient in Okinawa trough sediments. *Archaea* **2016**, 1–12 (2016).
33. Labonté, J. M., Lever, M. A., Edwards, K. J. & Orcutt, B. N. Influence of igneous basement on deep sediment microbial diversity on the Eastern Juan de Fuca Ridge Flank. *Front. Microbiol.* **8**, 1434 (2017).
34. Inagaki, F. et al. Exploring deep microbial life in coal-bearing sediment down to ~2.5 km below the ocean floor. *Science* **349**, 420–424 (2015).
35. Huber, J. A., Johnson, H. P., Butterfield, D. A. & Baross, J. A. Microbial life in ridge flank crustal fluids. *Environ. Microbiol.* **8**, 88–99 (2006).
36. Meyer, J. L. et al. A distinct and active bacterial community in cold oxygenated fluids circulating beneath the western flank of the Mid-Atlantic ridge. *Sci. Rep.* **6**, 1–14 (2016).
37. Tully, B. J., Wheat, C. G., Glazer, B. T. & Huber, J. A. A dynamic microbial community with high functional redundancy inhabits the cold, oxic subseafloor aquifer. *ISME J.* **12**, 1–16 (2018).
38. Blair, C. C., D'Hondt, S., Spivack, A. J. & Kingsley, R. H. Radiolytic hydrogen and microbial respiration in subsurface sediments. *Astrobiology* **7**, 951–970 (2007).
39. Dzaugis, M. E., Spivack, A. J., Dunlea, A. G., Murray, R. W. & D'Hondt, S. Radiolytic hydrogen production in the subseafloor basaltic aquifer. *Front. Microbiol.* **7**, 76 (2016).
40. Gieskes, J. M. Chemistry of interstitial waters of marine sediments. *Annu. Rev. Earth Planet. Sci.* **3**, 433–453 (1975).
41. Froelich, P. N. et al. Early oxidation of organic matter in pelagic sediments of the eastern equatorial Atlantic: suboxic diagenesis. *Geochim. et. Cosmochim. Acta* **43**, 1075–1090 (1979).
42. Bekins, B. A., Gody, E. M. & Warren, E. Distribution of microbial physiologic types in an aquifer contaminated by crude oil. *Microb. Ecol.* **37**, 263–275 (1999).
43. Barnes, R. O. & Goldberg, E. D. Methane production and consumption in anoxic marine sediments. *Geology* **4**, 297–300 (1976).
44. Schrum, H. N., Spivack, A. J., Kastner, M. & D'Hondt, S. Sulfate-reducing ammonium oxidation: A thermodynamically feasible metabolic pathway in subseafloor sediment. *Geology* **37**, 939–942 (2009).
45. Hinrichs, K. U. et al. Biological formation of ethane and propane in the deep marine subsurface. *Proc. Natl Acad. Sci. USA* **103**, 14684–14689 (2006).
46. Teske, A., Biddle, J. F. & Lever, M. A. Genetic Evidence of Subseafloor Microbial Communities. in *Earth and life processes discovered from subseafloor environments: A decade of science achieved by the Integrated Ocean Drilling Program (IODP)* 85–125 (Elsevier, 2014).
47. Hayes, J. M. & Waldbauer, J. R. The carbon cycle and associated redox processes through time. *Philos. Trans. R. Soc. Lond. Ser. B, Biol. Sci.* **361**, 931–950 (2006).
48. Schlesinger, W. H. & Bernhardt, E. S. *Biogeochemistry: an analysis of global change*. (Academic Press, 2013).
49. Pilson, M. E. Q. *An introduction to the chemistry of the sea*. (Cambridge University Press, 2013).
50. Gruber, N. *The Marine Nitrogen Cycle: Overview and Challenges, In Nitrogen in the Marine Environment*. (Academic Press, 2008).
51. Head, I. M., Jones, D. M. & Larter, S. R. Biological activity in the deep subsurface and the origin of heavy oil. *Nature* **426**, 344–352 (2003).
52. Crosby, C. H. & Bailey, J. V. The role of microbes in the formation of modern and ancient phosphatic mineral deposits. *Front. Microbiol.* **3**, 241 (2012).
53. Moore, T. S., Murray, R. W., Kurtz, A. C. & Schrag, D. P. Anaerobic methane oxidation and the formation of dolomite. *Earth Planet. Sci. Lett.* **229**, 141–154 (2004).
54. Meister, P. et al. Dolomite formation in the dynamic deep biosphere: Results from the Peru Margin. *Sedimentology* **54**, 1007–1032 (2007).
55. Paytan, A., Mearon, S., Cobb, K. & Kastner, M. Origin of marine barite deposits: Sr and S isotope characterization. *Geology* **30**, 747–750 (2002).
56. Kendall, B., Anbar, A. D., Kappler, A. & Konhauser, K. O. The Global Iron Cycle. in *Fundamentals of Geobiology* 65–92 (John Wiley & Sons, Ltd, 2012).
57. Lyons, T. W., Reinhard, C. T. & Planavsky, N. J. The rise of oxygen in Earth's early ocean and atmosphere. *Nature* **506**, 307–315 (2014).
58. Hedges, S., Blair, J. E., Venturi, M. L. & Shoe, J. L. A molecular timescale of eukaryote evolution and the rise of complex multicellular life. *BMC Evolutionary Biology* **4**, 1–9 (2004).
59. Jiang, Y.-Y., Kong, D.-X., Qin, T. & Zhang, H. Y. How does oxygen rise drive evolution? Clues from oxygen-dependent biosynthesis of nuclear receptor ligands. *Biochem. Biophys. Res. Commun.* **391**, 1158–1160 (2010).
60. Hazen, R. M. et al. Mineral evolution. *Am. Mineral.* **93**, 1693–1720 (2008).
61. Sarmiento, J. L. & Gruber, N. *Ocean biogeochemical dynamics*. (Princeton University Press, 2006).
62. Field, C. B., Behrenfeld, M. J., Randerson, J. T. & Falkowski, P. Primary production of the biosphere: Integrating terrestrial and oceanic components. *Science* **281**, 237–240 (1998).
63. Dunne, J. P., Sarmiento, J. L. & Gnanadesikan, A. A synthesis of global particle export from the surface ocean and cycling through the ocean interior and on the seafloor. *Global Biogeochemical Cycles* **21**, 1–16 (2007).
64. Anderson, L. A. & Sarmiento, J. L. Redfield ratios of remineralization determined by nutrient data analysis. *Glob. Biogeochem. Cycles* **8**, 65–80 (1994).
65. Burdige, D. J. Geochemistry of marine sediments. in *Eos, Transactions American Geophysical Union* (Princeton University Press, 2006).
66. Orcutt, B. N. et al. Oxygen consumption rates in subseafloor basaltic crust derived from a reaction transport model. *Nature Communications* **4**, 1–8 (2013).
67. Canfield, D. E., Kristensen, E. & Thamdrup, B. Aquatic geomicrobiology. in *Advances in marine biology* (Academic Press, 2005).
68. Baquira, J. P. M. et al. Temperature and redox effect on mineral colonization in Juan de Fuca ridge flank subsurface crustal fluids. *Front. Microbiol.* **7**, 396 (2016).
69. Smith, A. R. et al. Deep crustal communities of the Juan de Fuca ridge are governed by mineralogy. *Geomicrobiol. J.* **34**, 147–156 (2017).
70. Jørgensen, B. B. Mineralization of organic matter in the sea bed—the role of sulphate reduction. *Nature* **296**, 643–645 (1982).
71. Wang, G., Spivack, A. J., Rutherford, S., Manor, U. & D'Hondt, S. Quantification of co-occurring reaction rates in deep subseafloor sediments. *Geochim. et. Cosmochim. Acta* **72**, 3479–3488 (2008).
72. Spivack, A. J. & Staudigel, H. Low-temperature alteration of the upper oceanic crust and the alkalinity budget of seawater. *Chem. Geol.* **115**, 239–247 (1994).
73. Knittel, K. & Boetius, A. Anaerobic oxidation of methane: progress with an unknown process. *Annu. Rev. Microbiol.* **63**, 311–334 (2009).
74. Gartman, A. et al. Microbes facilitate mineral deposition in bioelectrochemical systems. *ACS Earth Space Chem.* **1**, 277–287 (2017).
75. Canfield, D. E. Factors influencing organic carbon preservation in marine sediments. *Chem. Geol.* **114**, 315–329 (1994).
76. Paraska, D. W., Hipsey, M. R. & Salmon, S. U. Sediment diagenesis models: Review of approaches, challenges and opportunities. *Environ. Model. Softw.* **61**, 297–325 (2014).
77. Hoehler, T. M., Alperin, M. J., Albert, D. B. & Martens, C. S. Apparent minimum free energy requirements for methanogenic Archaea and sulfate-reducing bacteria in an anoxic marine sediment. *FEMS Microbiol. Ecol.* **38**, 33–41 (2001).
78. Jin, Q. & Bethke, C. M. Cellular energy conservation and the rate of microbial sulfate reduction. *Geology* **37**, 1027–1030 (2009).
79. Einstein, A. Über die von der molekularkinetischen Theorie der Wärme geforderte Bewegung von in ruhenden Flüssigkeiten suspendierten Teilchen. *Ann. der Phys.* **322**, 549–560 (1905).
80. Mahmoudi, N., Beaupré, S. R., Steen, A. D. & Pearson, A. Sequential bioavailability of sedimentary organic matter to heterotrophic bacteria. *Environ. Microbiol.* **19**, 2629–2644 (2017).
81. Mayer, L. M. Sedimentary organic matter preservation: an assessment and speculative synthesis—a comment. *Mar. Chem.* **49**, 123–126 (1995).
82. Petsch, S. T., Eglinton, T. I. & Edwards, K. J. ¹⁴C-Dead living biomass: evidence for microbial assimilation of ancient organic carbon during shale weathering. *Science* **292**, 1127–1131 (2001).
83. Steen, A. D. & Arnosti, C. Picky, hungry eaters in the cold: persistent substrate selectivity among polar pelagic microbial communities. *Frontiers in Microbiology* **5**, 1–5 (2014).
84. Meyers, P. A. Preservation of elemental and isotopic source identification of sedimentary organic matter. *Chem. Geol.* **114**, 289–302 (1994).
85. Estes, E. R. et al. Persistent organic matter in oxic subseafloor sediment. *Nat. Geosci.* **12**, 126–131 (2019).
86. Wehrmann, L. M. et al. Coupled organic and inorganic carbon cycling in the deep subseafloor sediment of the northeastern Bering Sea Slope (IODP Exp. 323). *Chem. Geol.* **284**, 251–261 (2011).
87. Mayer, L. M. Surface area control of organic carbon accumulation in continental shelf sediments. *Geochim. et. Cosmochim. Acta* **58**, 1271–1284 (1994).
88. Hedges, J. I. & Keil, R. G. Sedimentary organic matter preservation: an assessment and speculative synthesis. *Mar. Chem.* **49**, 81–115 (1995).
89. Pedersen, T. F. Sedimentary organic matter preservation: an assessment and speculative synthesis—a comment. *Mar. Chem.* **49**, 117–119 (1995).
90. Ransom, B., Bennett, R. H., Baerwald, R. & Shea, K. TEM study of in situ organic matter on continental margins: occurrence and the “monolayer” hypothesis. *Mar. Geol.* **138**, 1–9 (1997).
91. Henrichs, S. M. Sedimentary organic matter preservation: an assessment and speculative synthesis—a comment. *Mar. Chem.* **49**, 127–136 (1995).

92. Jarrard, R. D., Abrams, L. J., Pockalny, R., Larson, R. L. & Hirono, T. Physical properties of upper oceanic crust: Ocean Drilling Program Hole 801 C and the waning of hydrothermal circulation. *J. Geophys. Res.: Solid Earth* **108**, 1–26 (2003).
93. Jørgensen, B. B. & Kasten, S. Sulfur cycling and methane oxidation. in *Marine Geochemistry* (eds. Schulz, H. D. & Zabel, M.) 271–309 (Springer, Berlin, 2006).
94. Bowles, M. W., Mogollón, J. M., Kasten, S., Zabel, M. & Hinrichs, K. U. Global rates of marine sulfate reduction and implications for sub-sea-floor metabolic activities. *Science* **344**, 889–891 (2013).
95. Starnawski, P. et al. Microbial community assembly and evolution in subseafloor sediment. *Proc. Natl Acad. Sci. USA* **114**, 2940–2945 (2017).
96. Kirkpatrick, J. B., Walsh, E. A. & D'Hondt, S. Microbial selection and survival in subseafloor sediment. *Proc. Natl Acad. Sci.* **10**, 1–15 (2019).
97. Heberling, C., Lowell, R. P., Liu, L. & Fisk, M. R. Extent of the microbial biosphere in the oceanic crust. *Geochem. Geophys. Geosyst.* **11**, 1–15 (2010).
98. Stein, C. A. & Stein, S. Constraints on hydrothermal heat flux through the oceanic lithosphere from global heat flow. *J. Geophys. Res.: Solid Earth* **99**, 3081–3095 (1994).
99. Hamza, V. M., Cardoso, R. R. & Ponte Neto, C. F. Spherical harmonic analysis of earth's conductive heat flow. *Int. J. Earth Sci.* **97**, 205–226 (2008).
100. Divins, D. L. Total Sediment Thickness of the World's Oceans and Marginal Seas. (2003). Available at: <https://www.ngdc.noaa.gov/mgg/sedthick/sedthick.html>. (Accessed 13th May 2018).
101. Becker, K. Measurements of the permeability of the sheeted dikes in Hole 504B. *ODP Leg.* **111**, 317–325 (1989).
102. IODP-MI. Scientific Earth Drilling Information Service - SEDIS. Available at: <http://sedis.iodp.org/>. (Accessed 13th May 2018)
103. Müller, R. D., Sdrolias, M., Gaina, C. & Roest, W. R. Age, spreading rates, and spreading asymmetry of the world's ocean crust. *Geochem. Geophys. Geosyst.* **8150**, (2008).
104. Schulz, H. D. Quantification of Early Diagenesis: Dissolved Constituents in Marine Pore Water. in *Marine Geochemistry* 85–128 (Springer Berlin Heidelberg, 2000).
105. Jansen, E. & Raymo, M. E. Leg 162: New Frontiers on Past Climates. *Proceedings of the Ocean Drilling Program, Initial Reports* **162**, (1996).
106. D'Hondt, S., Jørgensen, B. B., Miller, D. J. & Al., E. ODP Leg 201. *Proceedings of the Ocean Drilling Program, Initial Reports* **201**, (2003).
107. D'Hondt, S., Inagaki, F., Alvarez Zarikian, C. A. & The Expedition 329 Scientists. Expedition 329, South Pacific Gyre Subseafloor Life. *Proceedings of the International Ocean Discovery Program* (2011).
108. Thauer, R. K., Jungermann, K. & Decker, K. Energy conservation in chemotrophic anaerobic bacteria. *Bacteriol. Rev.* **41**, 100–180 (1977).
109. Schink, B. Energetics of syntrophic cooperation in methanogenic degradation. *Microbiol. Mol. Biol. Rev.* **61**, 262–280 (1997).
110. Harder, J. Species-independent maintenance energy and natural population sizes. *FEMS Microbiol. Ecol.* **23**, 39–44 (1997).
111. Wang, G., Spivack, A. J. & D'Hondt, S. Gibbs energies of reaction and microbial mutualism in anaerobic deep subseafloor sediments of ODP Site 1226. *Geochim. et. Cosmochim. Acta* **74**, 3938–3947 (2010).
112. Boudart, M. Consistency between kinetics and thermodynamics. *J. Phys. Chem.* **80**, 2869–2870 (1976).
113. Dale, A. W. et al. Seasonal dynamics of the depth and rate of anaerobic oxidation of methane in Aarhus Bay (Denmark) sediments. *J. Mar. Res.* **66**, 127–155 (2008).
114. Lovley, D. R. & Phillips, E. J. Organic matter mineralization with reduction of ferric iron in anaerobic sediments. *Appl. Environ. Microbiol.* **51**, 683–689 (1986).
115. Engelen, B. et al. Fluids from the Oceanic Crust support microbial activities within the deep biosphere. *Geomicrobiol. J.* **25**, 56–66 (2008).
116. Buchwald, C. et al. Isotopic constraints on nitrogen transformation rates in the deep sedimentary marine biosphere. *Glob. Biogeochem. Cycles* **32**, 1688–1702 (2018).
117. Wehrmann, L. M. et al. Iron-controlled oxidative sulfur cycling recorded in the distribution and isotopic composition of sulfur species in glacially influenced fjord sediments of west Svalbard. *Chem. Geol.* **466**, 678–695 (2017).
118. Bethke, C. M., Ding, D., Jin, Q. & Sanford, R. A. Origin of microbiological zonation in groundwater flows. *Geology* **36**, 739–742 (2008).
119. Cohen, E. R. et al. *Quantities, Units and Symbols in Physical Chemistry, IUPAC Green Book.* (eds. Cohen, E. R. et al.) (RSC Publishing, 2008).

Acknowledgements

We thank Timothy Ferdelman and Richard W. Murray for helpful comments. We thank Josh Wood of the Deep Carbon Observatory for assistance with figures. This project was funded by the US National Science Foundation (through grant NSF-OCE-1130735 and the Center for Deep Dark Energy Biosphere Investigations [grant NSF-OCE-0939564]) and the National Aeronautics and Space Administration (grant NNX12AD65G). This is a contribution to the Deep Carbon Observatory (DCO). It is Center for Dark Energy Biosphere Investigations (C-DEBI) publication 454.

Author contributions

S.D. wrote the manuscript, with input from R.P., V.F. and A.J.S. R.P. created the global maps. V.F. and R.P. calculated vertical distributions of net respiration rates. S.D. and A.J.S. calculated global fluxes and developed the model of organic oxidation rate as a function of reaction affinity and diffusive distance. All authors provided editorial comments on the manuscript.

Additional information

Competing interests: The authors declare no competing interests.

Reprints and permission information is available online at <http://npg.nature.com/reprintsandpermissions/>

Peer review information: *Nature Communication* would like to thank Wolfgang Bach and Peter Girguis for their contributions to the peer review of this work.

Publisher's note: Springer Nature remains neutral with regard to jurisdictional claims in published maps and institutional affiliations.



Open Access This article is licensed under a Creative Commons Attribution 4.0 International License, which permits use, sharing, adaptation, distribution and reproduction in any medium or format, as long as you give appropriate credit to the original author(s) and the source, provide a link to the Creative Commons license, and indicate if changes were made. The images or other third party material in this article are included in the article's Creative Commons license, unless indicated otherwise in a credit line to the material. If material is not included in the article's Creative Commons license and your intended use is not permitted by statutory regulation or exceeds the permitted use, you will need to obtain permission directly from the copyright holder. To view a copy of this license, visit <http://creativecommons.org/licenses/by/4.0/>.

© The Author(s) 2019